Zirconium-Assisted Aldol Condensation Reactions of Amido Enolates: Structural and Kinetic Analysis of the Reaction of *N,N*-Diphenylacetamide and *N,N*-Diphenylpropionamide Enolates with Benzaldehyde and *p*-Substituted Acetophenones

Pier Giorgio Cozzi,† Patrick Veya, and Carlo Floriani*

Institut de Chimie Minérale et Analytique, BCH, Université de Lausanne, CH-1015 Lausanne, Switzerland

François P. Rotzinger

Institut de Chimie Physique, Ecole Polytechnique Fédérale, CH-1015 Lausanne, Switzerland

Angiola Chiesi-Villa and Corrado Rizzoli

Dipartimento di Chimica, Universitá di Parma, I-43100 Parma, Italy

Received June 27, 1995[⊗]

The deprotonation of *N,N*-diphenyl amides with LDA and subsequent reaction with $[(cp)_2ZrCl_2]$ (cp = η^5-C_5H_5) allowed the enolate complexes $[\{Ph_2NC(CH_2)O\}Zr(cp)_2(Cl)]$ (**5**) and $[\{Ph_2NC(CHCH_3)O\}Zr(cp)_2(Cl)]$ (**6**) to be isolated. The crystal structure of **6** is reported. Reaction of **5** with $[Cr(CO)_5]$·THF gave $[Ph_2NC\{CH_2Cr(CO)_5\}\{OZr(Cl)(cp)_2\}]$ (**7**), an O- and C-bonded dimetallic amido enolate. Reaction of **5** and **6** with benzaldehyde gave the corresponding aldol products **8** and **9**; according to previous reports, the conversion of **6** into **9** is *syn* selective. Reaction of **6** with acetophenone followed by addition of silver triflate gave the complex $[Ph_2NC(=O)CH(CH_3)C(Me)(Ph)OZr(cp)_2(Cl)(OSO_2CF_3)]$ (**11**) as a diastereoisomeric mixture in the ratio *anti*:*syn* = 65:35. The crystal structure of *syn*-**11** is reported. This cyclic complex mimics the postulated cyclic transition state of the aldol reaction mediated by zirconium amide enolates. A kinetic investigation of the reaction of **6** with acetophenone was performed and gave the following activation parameters: $\Delta H^{\ddagger} = 38.3 \pm 0.9$ kJ mol^{-1}; $\Delta S^{\ddagger} \geq -181 \pm 3$ J mol^{-1} K^{-1}; $\Delta G^{\ddagger}_{298} = 92.2 \pm 1.2$ kJ mol^{-1}. A similar study with 4-fluoroacetophenone gave $\Delta H^{\ddagger} = 43.5 \pm 1.3$ kJ mol^{-1}, $\Delta S^{\ddagger} \geq -167 \pm 4$ J mol^{-1} K^{-1}, and $\Delta G^{\ddagger}_{298} = 93.3 \pm 1.8$ kJ mol^{-1}. The reaction rate at 320 K determined with 4-chloro-, 4-methyl-, and 4-nitroacetophenone allowed the determination of a Hammett plot with $\varrho = 0.41$. This value is implicit of a carbon–carbon bond-forming, rate-limiting step.

Introduction

Amide enolates are of great synthetic importance, particularly with regard to highly selective carbon–carbon bond formation.[1] For example, their conversion into β-hydroxy carbonyls represents a convenient route to the building blocks of polypropionate- and polyacetate-derived natural products.[2] Despite such widespread use, however, structural information is sparse.[3] Although structural studies have been reported for some lithium amide enolates,[4] no previous study of transition-metal analogues has been published.[5]

Boron enolates have been subjected to *ab initio* calculations,[6] and a related force field study[7] has helped shed light on the aldolic reaction mediated by boron. However, the difficulties encountered in developing an *ab initio* approach for transition-metal complexes are well-known. Consequently, theoretical analysis of transition-metal amide enolates has only been performed at a primitive level.[8] For transition-metal enolate complexes, simple and facial stereoselection are currently interpreted by a hypothetical model derived from study-

* To whom correspondence should be addressed.
† Present address: Istituto di Chimica "G. Ciamician", Università di Bologna, I-40216 Bologna, Italy.
⊗ Abstract published in *Advance ACS Abstracts,* August 1, 1995.

(1) Heathcock, C. H. In *Comprehensive Organic Synthesis*; Heathcock, C. H., Ed.; Pergamon: Oxford, U.K., 1991; Vol. 2, p 181. Kim, M. B.; Williams, S. F.; Masamune, S. In *Comprehensive Organic Synthesis*; Heathcock, C. H., Ed.; Pergamon: Oxford, U.K., 1991; Vol. 2, p 239. Oare, D. A.; Heathcock, C. H. In *Topics in Stereochemistry*; Eliel, E. L., Wilen, S. H., Eds.; Wiley: New York, 1989; p 227.

(2) *Polyether Antibiotics*; Wesley, J. W., Ed.; Marcel Dekker: New York, 1982. *Macrolide Antibiotics*; Omura, S., Ed.; Academic: Orlando, FL, 1984. Paterson, I.; Mansury, M. M. *Tetrahedron* **1985**, *41*, 3569. Boeckman, R. H.; Goldstein, M. In *The Total Synthesis of Natural Products*; Wiley: New York, 1988. Tatsuta, K. In *Recent Progress in the Chemical Synthesis of Antibiotics*; Springer: Berlin, Germany, 1990. Nakata, M.; Tatsuta, K. In *Studies in Natural Product Chemistry*; Rahman, A. U., Ed.; Elsevier: Amsterdam, Holland, 1993; Vol. 12, part 4.

(3) Williard, P. G. In *Comprehensive Organic Synthesis*; Schreiber, S. L., Ed.; Pergamon: Oxford, England, 1991; Vol. 1, p 1. Seebach, D. *Angew. Chem., Int. Ed. Engl.* **1988**, *27*, 1624. Cieplak, A. S. In *Structure Correlation*; Bürgi, H.-B.; Dunitz, J. D., Eds.; VCH: New York, 1994; p 205.

(4) Laube, T.; Dunitz, J. D.; Seebach, D. *Helv. Chim. Acta* **1985**, *68*, 1373. Buaer, W.; Laube, T.; Seebach, D. *Chem. Ber.* **1985**, *118*, 764.

(5) Veya, P.; Floriani, C.; Chiesi-Villa, A.; Rizzoli, C. *J. Chem. Soc., Chem. Commun.* **1991**, 1166.

(6) Li, Y.; Paddon-Row, M. N.; Houk, K. N. *J. Am. Chem. Soc.* **1988**, *110*, 3684. Li, Y.; Paddon-Row, M. N.; Houk, K. N. *J. Org. Chem.* **1990**, *55*, 481. Bernardi, F.; Robb, M. A.; Suzzi-Valli, G.; Tagliavini, E.; Umani-Ronchi, A. *J. Org. Chem.* **1991**, *56*, 6472.

(7) Bernardi, A.; Capelli, A. M.; Gennari, C.; Goodman, J. M.; Paterson, I. *J. Org. Chem.* **1990**, *55*, 3576. Vulpetti, A.; Bernardi, A.; Gennari, C.; Goodman, J. M.; Paterson, I. *Tetrahedron* **1993**, *49*, 685.

0276-7333/95/2314-4092$09.00/0

Scheme 1

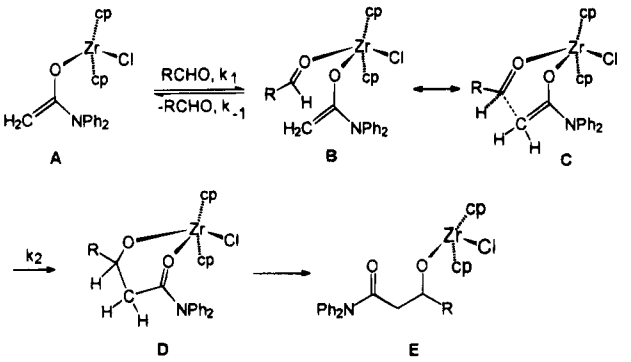

ing the scope of the reaction in connection with Hoffmann's analysis of the frontier orbitals available for a bent metallocene fragment.[9] It is therefore desirable to obtain accurate structural information for such complexes. The bond parameters observed should be of particular use in deciding the role of sterically bulky substituents in determining stereoselectivity. Moreover, although a detailed force field calculation is presently beyond us, the bond lengths and angles recorded may be of use for future studies in this area.

Therefore, we now report the synthesis and characterization of two zirconocene amido enolate complexes which we used in reactions with carbonyl compounds.[10] The X-ray structure determination of the starting zirconium enolate and a derivative of the final product allows us to support the mechanism accepted for transition-metal-mediated aldol reactions, as indicated in Scheme 1.

Furthermore, kinetic analysis of a stereogenic amido enolate reacting with a range of *p*-substituted acetophenones has allowed us to calculate activation parameters and derive a Hammett plot. These latter data have showed that the rate-determining step for the aldol reaction involves the formation of a carbon−carbon bond.

Results and Discussion

Deprotonation of *N,N*-diphenylacetamide (**1**) and *N,N*-diphenylpropionamide (**2**) was carried out according to Scheme 2. As shown by the ^{1}H NMR spectrum, the lithium enolate **3** possesses two molecules of THF bound to the alkali-metal center and we therefore propose a dimeric structure with tetracoordinate lithium atoms. The ^{1}H NMR spectrum of **3** includes singlets at 3.42 and 3.63 ppm, which are assigned to the enolic protons: these chemical shifts fall within the range of previously reported data for unsolvated enolates.[11]

The *in situ* generation of **3** and **4** was followed by transmetalation with $(cp)_2ZrCl_2$ at low temperature. Slow warming to room temperature and appropriate workup procedures led to the isolation of **5** and **6** (Scheme 2). The corresponding reaction with $(cp)_2TiCl_2$ gave products which could not be isolated without decomposition.[12] Nonetheless, although they are highly

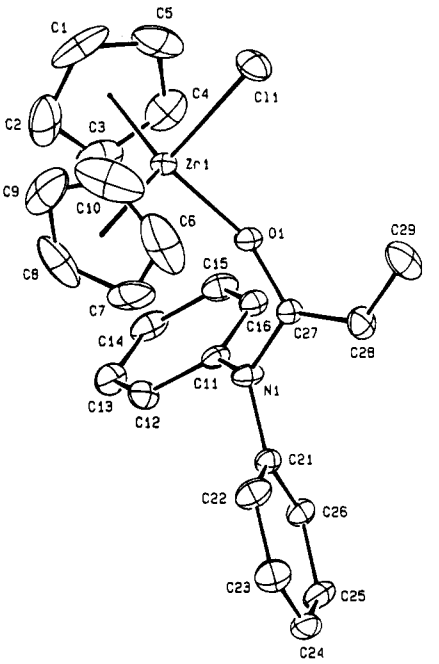

Figure 1. ORTEP drawing for complex **6** (30% ellipsoids).

Scheme 2

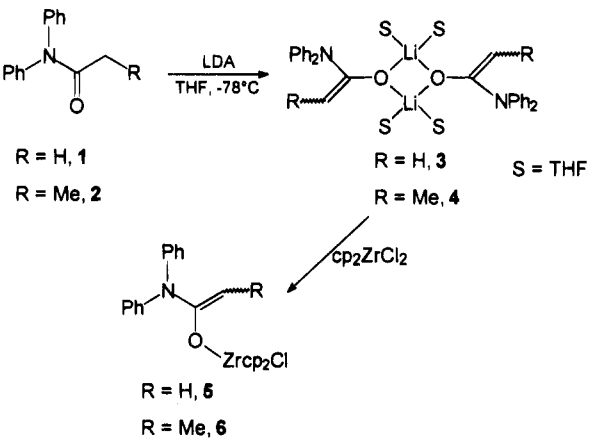

susceptible to moisture, both **5** and **6** are yellow solids stable at room temperature under an inert atmosphere.

Isolation of **6** directly from the reaction mixture gave a 65:35 mixture of diastereoisomers; attempts to separate these by recrystallization failed, with the original ratio unchanged. Structural analysis on an X-ray-quality crystal of **6** allowed us to determine the bond connectivity and parameters of the *Z* isomer. The structure of **6** is shown in Figure 1, while a selection of bond distances and angles is given in Table 2. Complex **6** is a monomer, with a geometry very close to the structure of nonstereogenic *N,N*-diphenyl amido enolates previously characterized.[5] Some differences are observed in the torsion angles, as indicated by the values reported in Table 2.

The dihedral angles of the C11···C16 and C21···C26 phenyl planes with respect to the enolato O1,N1,C27,-C28 plane are very close in both complexes (111.5(1) and 104.7(1)°, respectively, for **6**; 112.5(1) and 109.5(2)° for **5**). The main feature of both structures is the disposition of the enolate carbon *syn* to Cl. One of the phenyls is *syn* to zirconium. The dihedral angle between Cl1−

(8) Paterson, I. In *Comprehensive Organic Synthesis*; Heathcock, C. H., Ed.; Pergamon: Oxford, U.K., 1991; Vol. 2, p 301.

(9) Evans, D. A.; McGee, R. *Tetrahedron Lett.* **1980**, *21*, 3975. Evans, D. A.; McGee, R. *J. Am. Chem. Soc.* **1981**, *103*, 2876.

(10) For previous study by our laboratory in this area: (a) Berno, P.; Floriani, C.; Chiesi-Villa, A.; Rizzoli, C. *Organometallics* **1990**, *9*, 1995. (b) Veya, P.; Cozzi, P. G.; Rotzinger, F.; Floriani, C.; Chiesi-Villa, A.; Rizzoli, C. *Organometallics* **1995**, *14*, 4101.

(11) Veya, P. Thèse de doctorat, University of Lausanne, Lausanne, Switzerland, 1993.

(12) Titanium enolates prepared *in situ* from pyrrolidinopropionamide react with aldehydes, giving *anti* products: Murphy, P. J.; Procter, G.; Russel, A. T. *Tetrahedron Lett.* **1987**, *28*, 2037.

Table 1. Experimental Data for the X-ray Diffraction Studies on Crystalline Compounds 6, 7, and 11

	6	7	11
formula	$C_{25}H_{24}ClNOZr$	$C_{29}H_{22}ClCrNO_6Zr$	$C_{34}H_{32}F_3NO_5SZr \cdot C_4H_8O$ (2/1)
a (Å)	10.636(1)	9.870(1)	18.368(5)
b (Å)	12.029(1)	23.237(2)	14.115(4)
c (Å)	9.405(1)	13.338(1)	14.398(4)
α (deg)	70.45(1)	90	90
β (deg)	77.97(1)	105.94(1)	109.08(4)
γ (deg)	76.37(1)	90	90
V (Å^3)	1093.6(2)	2941.4(5)	3527.8(19)
Z	2	4	4
fw	481.1	659.2	751.0
space group	$P\bar{1}$ (No. 2)	Cc (No. 9)	$P2_1/n$ (No. 14)
t (°C)	22	22	22
λ (Å)	0.71069	0.71069	0.71069
ϱ_{calc} (g cm^{-3})	1.461	1.489	1.414
μ (cm^{-1})	6.41	8.55	4.19
transmission coeff	0.985–1.00	0.937–1.000	0.952–1.000
R^a	0.026	0.026 [0.027][c]	0.058
R_G[b]		0.028 [0.029]	

[a] $R = \Sigma||\Delta F|/\Sigma|F_o|$. [b] $R_G = [\Sigma w|\Delta F|^2/\Sigma w|F_o|^2]^{1/2}$. [c] Values in brackets refer to the "inverted" structure.

Zr–O1 and O1–C27–C28 varies from 30.0(1)° in **6** to 33.8(3)° in **5**. The angles Zr–O–C11 (19.2(3)°) and Cl1–Zr–C11 (−179.4(2)°) show the *Z* configuration of the enolate in **6**. The C27–C28 bond distances in **5**[5] and **6** confirm the presence of a localized double bond.

However, despite a full characterization of **6**, assignment of configuration to the major and minor components of the diastereoisomeric mixture was not directly possible. A ^{1}H NMR NOESY experiment suggested that the major component has a *Z* configuration, but this was no conclusive. Nevertheless, indirect evidence firmly supports the *Z* isomer as the most abundant diastereoisomer. First, it is well-established that hindered amides favor the formation of *Z* enolates.[1] Furthermore, the ^{1}H NMR chemical shift of the most intense methyl signal correlates closely with related *Z* enolates reported previously.[9]

The reaction of **5** and **6** with carbonyl compounds probably proceeds according to the pathway in Scheme 1, where the metal plays the role of templating agent. We envisaged, however, a number of reactions where the zirconium-nonassisted nucleophilic reactivity of the enolate can lead to novel organometallic bifunctional species. This is exemplified in the reaction of **5** with the soft electrophile [Cr(CO)$_5$(THF)].

The reaction in Scheme 3 exemplifies the preliminary attack of the enolate nucleophile at an electrophilic center, and this is not followed by an evolution of the nucleophile–electrophile adduct. Such a reaction was successful only with the most strongly nucleophilic enolates, such as the amido enolates, while it was not observed with the ketone enolates. The strong electronic influence of the [Cr(CO)$_5$] fragment affects the chemical shifts of the methylene group. The proposed bonding scheme of compound **7** is supported by the structural data in Table 2, which were obtained from a single crystal X-ray analysis.

In complex **7** the enolato fragment has a geometry close (see Figure 2) to that observed in complexes **5** and **6**. Also in this case the nucleophilic CH_2 is *syn* to N1 and *trans* with respect to the Cl1 ligand at zirconium, as indicated by the value of the torsional angles Cl1–Zr···C27–N1 and Cl1–Zr···C27–C28 (Table 2). The orientation of the phenyl rings is similar to that observed in complex **6**, the dihedral angles of the C11···C16 and C21···C26 phenyl planes with respect to the enolato O1,N1,C27,C28 plane being 109.8(1) and 101.9(1)°. The binding of [Cr(CO)$_5$] induces a specific rotation around the Zr–O bond, as indicated by the values of the Cl1–Zr–O1–C27, Zr–O1–C27–C28, and Zr–O1–C27–N1 torsional angles. The CH_2 nucleophile binds Cr at a normal distance for a Cr–C σ bond (2.328(5)°). The CO *trans* to it takes care of the major amount of the charge transferred by the enolate to the metal, the Cr–C33 (1.814(5) Å) and C33–O33 (1.66(7) Å) being significantly shorter and longer, respectively, than those found for the other four Cr–CO groups (mean values: Cr–C, 1.898(8) Å; C–O, 1.139(10) Å). Lengthening of the C27–C28 and Zr–O1 bonds and shortening of the C27–O1 and N1–C27 bonds were observed on moving from complexes **6** and **5** to **7** (see Table 2). This is in agreement with a partial electronic transfer at the intermediate stage by nucleophilic attack at an electrophile, before further reaction. The choice of metal carbonyls in the reaction with nucleophilic metal enolates was made because they contain two different electrophilic sites, namely the metal center in the case of coordinatively unsaturated metal carbonyls and the CO ligands in the case of coordinatively saturated metal carbonyls. The former reaction leads, as in the present case, to the formation of a O- and C-bonded dimetallic enolate, the chemistry of which is under investigation. In the latter case the attack by the enolate at the metal-bonded CO led to a novel class of dimetallocarbene.[13]

We were unable to identify any interesting reactivity behavior of **7**. Enolates **5** and **6** react cleanly with benzaldehyde to give extremely soluble oily products which we have not been able to crystallize. The reaction can be conveniently monitored using ^{1}H NMR in a sealed tube, and spectroscopic data for **8** and **9** (Scheme 4) are reported in the Experimental Section. In both products zirconium is now bonded to the oxygen derived from the carbonyl substrate.

Complex **8** displays characteristic ABX methylene signals at 2.42, 2.93, and 5.90 ppm (respective coupling constants of 3.5, 9.2, and 15.35 Hz). It is reassuring to note that these coupling constants are very close to those we found for cationic aldolato complexes with the metallacycle structure reported below, which we believe to be structural models for the aldol reaction transition state.[10] The aldol product **9** was found to be a mixture of diastereoisomers in an 81:19 ratio. Hydrolysis showed that the *syn* isomer is the most abundant one.[9]

(13) Veya, P.; Floriani, C.; Chiesi-Villa, A.; Rizzoli, C. *Organometallics* **1994**, *13*, 214.

Table 2. Selected Bond Distances (Å) and Angles (deg)

Complexes **6**, **7**, and **11**

	6	**7**	**11**
Within the Zirconium Coordination Sphere[a]			
Zr1–X	2.475(1)	2.415(2)	1.947(7)
Zr1–O1	1.981(2)	2.046(3)	2.239(7)
Zr1–cp1	2.230(4)	2.202(5)	2.259(16)
Zr1–cp2	2.215(7)	2.206(6)	2.267(15)
cp1–Zr1–cp2	129.2(2)	130.2(3)	123.9(5)
cp1–Zr1–X	106.5(1)	106.2(1)	118.4(4)
cp1–Zr1–O1	106.2(1)	108.2(2)	94.8(4)
cp2–Zr1–X	105.1(2)	106.8(2)	117.7(4)
cp2–Zr1–O1	106.8(2)	103.4(2)	97.5(4)
X–Zr1–O1	99.0(1)	97.3(1)	75.4(3)
Within the Ligands			
O1–C27	1.346(3)	1.310(5)	1.258(13)
N1–C27	1.424(3)	1.361(6)	1.337(13)
N1–C11	1.429(4)	1.423(5)	1.431(9)
N1–C21	1.438(3)	1.427(5)	1.432(10)
C27–C28	1.335(4)	1.385(7)	1.500(14)
C28–C29	1.487(5)		1.486(16)
X–C29			1.431(13)
Zr1–O1–C27	151.0(2)	141.1(3)	134.2(7)
Zr1–X–C29			145.8(7)
C27–N1–C11	117.9(2)	122.1(4)	119.8(8)
C27–N1–C21	118.9(2)	120.6(4)	123.4(8)
C11–N1–C21	117.2(2)	117.2(3)	116.7(8)
O1–C27–N1	112.4(2)	114.2(4)	118.1(10)
O1–C27–C28	124.1(3)	122.1(4)	122.6(10)
N1–C27–C28	123.4(3)	123.7(5)	119.2(10)
C27–C28–C29	124.9(3)		113.8(10)

Complex **7**

In the Coordination Sphere			
Cr1–C28	2.328(5)	O29–C29	1.146(7)
Cr1–C29	1.895(5)	O30–C30	1.131(11)
Cr1–C30	1.895(8)	O31–C31	1.135(11)
Cr1–C31	1.896(8)	O32–C32	1.144(12)
Cr1–C32	1.907(9)	O33–C33	1.166(7)
Cr1–C33	1.814(5)		
C28–Cr1–C33	173.6(2)	C31–Cr1–C32	93.2(3)
C29–Cr1–C31	175.5(3)	Cr1–C29–O29	172.7(5)
C30–Cr1–C32	174.5(3)	Cr1–C30–O30	174.5(7)
C29–Cr1–C30	84.4(3)	Cr1–C31–O31	176.5(8)
C29–Cr1–C32	90.1(3)	Cr1–C32–O32	176.1(6)
C30–Cr1–C31	92.2(4)	Cr1–C33–O33	177.6(5)

Torsional Angles for the Metal Enolate Fragment in **5**–**7**

	5	**6**	**7**
Cl1–Zr··C27–N1	176.7(3)	179.4(2)	181.7(4)
Cl1–Zr··C27–C28	18.4(4)	19.2(3)	23.1(3)
Zr–O1–C27–C28	−87.4(7)	−95.4(4)	−61.3(7)
Zr–O1–C27–N1	90.6(6)	83.1(4)	119.3(4)
Cl1–Zr–O1–C27	95.9(5)	104.9(4)	76.2(5)

[a] X = Cl1 for complexes **6** and **7**; X = O2 for complex **11**. Cp1 and Cp2 refer to the centroids of the cyclopentadienyl rings C1–C5 and C6–C10, respectively.

Applying the Karplus equation[14] to the NMR data for complex **8** (*i.e.* correlating coupling constants to dihedral angles between H_A, H_B, and H_X) allowed us to derive the following Newman projection to represent the favored solution conformation:

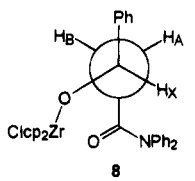

8

We believe that this is probably similar to the solid-state situation, because the bulky nature of the amide nitrogen substituents will hinder rotation around the newly formed carbon–carbon bond.[10] The steric encumbrance also serves to place the two oxygen atoms in a synclinal position. Although this orientation can be explained on steric grounds, it is worthy noting that this conformation can be derived from a cyclic transition state.[15]

The high rate of reaction of **5** with benzaldehyde and with acetophenone precluded a kinetic analysis of the

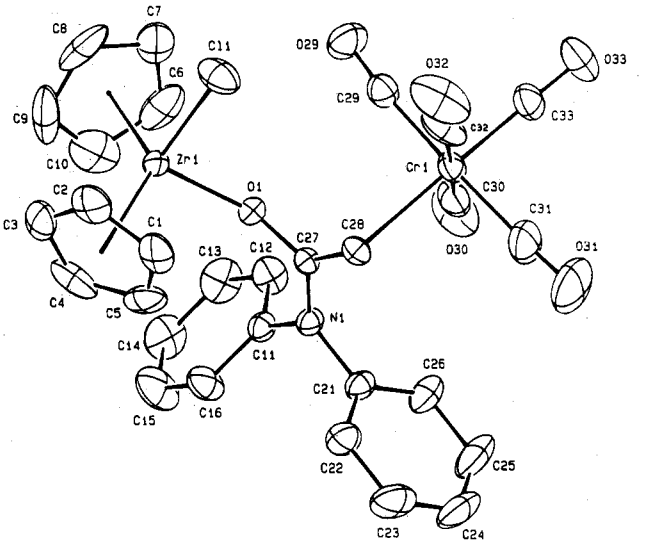

Figure 2. ORTEP drawing for complex **7** (30% ellipsoids).

Scheme 3

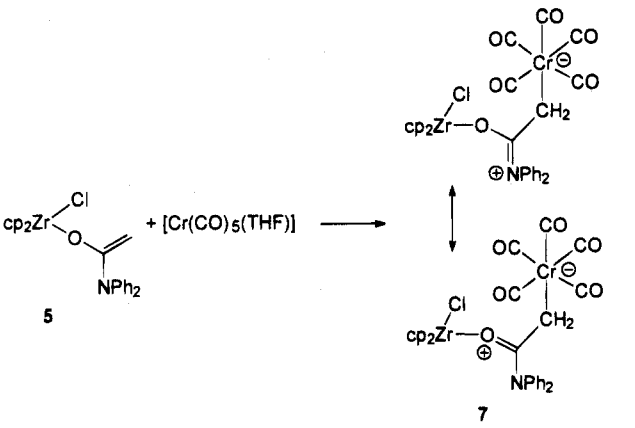

Scheme 4

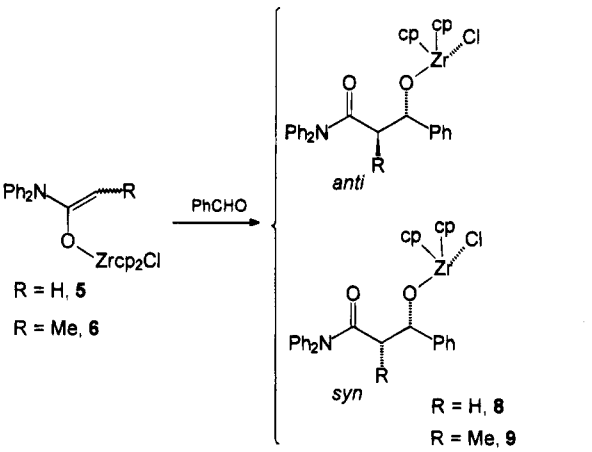

(14) (a) Pretsch, E.; Seibl, J.; Simon, W.; Clerc, T. *Tables of Spectral Data for Structure Determination of Organic Compounds*; Springer: Berlin, Germany, 1983. (b) Fleming, I.; Williams, D. H. *Spectroscopic Methods in Organic Chemistry*, 3rd ed.; McGraw-Hill: New York, 1980; p 100.

(15) Zimmerman, H. E.; Traxler, M. D. *J. Am. Chem. Soc.* **1957**, *79*, 1920.

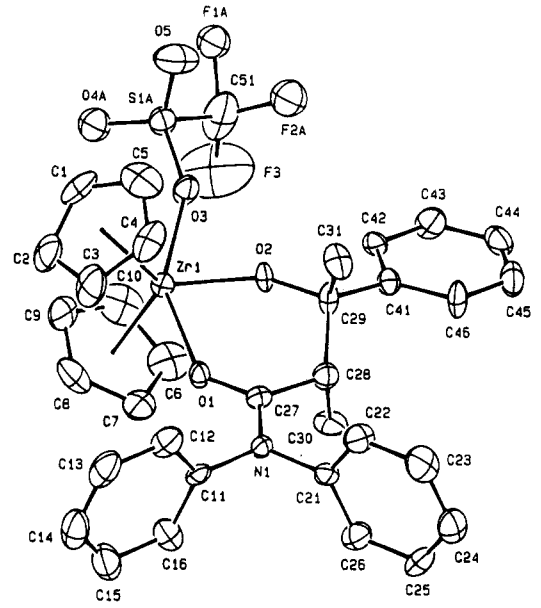

Figure 3. ORTEP drawing for complex **11** (30% ellipsoids). Only the A positions are given for the disordered S1, O4, F1, and F2 atoms.

Scheme 5

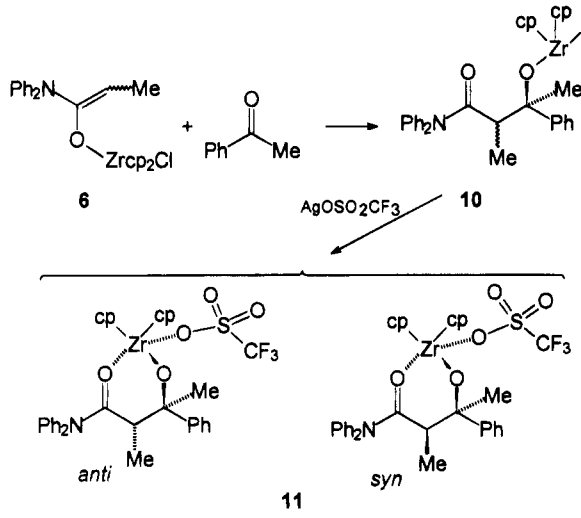

aldolic reaction. However, the reaction of **6** with acetophenone (to give **10** as a 65:35 diastereoisomeric mixture) proceeds more slowly at a rate amenable to a kinetic study by ^{1}H NMR (Scheme 5). Complex **10** is an oil but can be converted to the solid aldol product **11** by reaction with silver(I) triflate (Scheme 5).

Complex **11** also exists as a diastereoisomeric mixture (ratio 65:35). Given the similar nature of the diastereoisomer ratios of **10** and **11**, we believe it is reasonable to assume that the reaction with silver triflate does not affect the configuration of the stereogenic centers. The diastereoisomers of **11** may be separated by recrystallization. An X-ray analysis on a crystal so obtained showed the presence of a *syn* configuration. However, the ^{1}H NMR spectrum of this sample corresponded to the minor component of the product mixture: i.e., **10** is a diastereoisomeric ratio of 65% *anti*, 35% *syn*.

In the structure of **11** the cationic aldolato metallacycle has a rather long distance interaction between the metal and the counteranion (Zr1–O3, 2.290(7) Å). The Zr1,O1,O2,O3 plane is perpendicular to the cp1–Zr–cp2 plane (dihedral angle 88.0(4)°). The narrow O1–Zr–O2 angle (75.4(3)°) allows the binding of the fifth ligand by the metal. This ligand slightly affects the structural parameters of the $(cp)_2Zr$ group, the Zr–cp bond distances being significantly longer (2.259(16), 2.267(15) Å) and the cp1–Zr–cp2 angle narrower (123.9(5)°) than in **6** and **7**. The bidentate O,O′ ligand gives rise to a six-membered metallacycle with a half-chair conformation, the C28 carbon being 0.464(11) Å out of the plane containing Zr,O1,O2,C27,C29 (maximum displacement 0.114(12) Å for C29). The structural parameters of the metallacycle are essentially in agreement with the proposed bonding scheme, though the C27–O1 and C27–N1 bond distances, along with the planarity of the O1,N1,C27,C28 fragment, suggest some delocalization over the O1–C27–N1 moiety. The C30 and C31 methyl carbons assume an *anti* conformation, the C31–C29–C28–C30 torsion angle being −169.4(9)°. It is worth mentioning at this stage the relevance of **11** with respect to the transition state of the aldol reaction.

An important difference between the ^{1}H NMR spectra of **10** and **11** is the inversion in chemical shifts of the α-methyl protons. Although we cannot explain this peculiar effect, it is intriguing to note that a similar phenomenon is not observed for the methine proton (see Experimental Section). We suggest that in the syn isomer the α-methyl substituent lies in a position subjected to a shielding effect associated with one of the amide nitrogen phenyl rings (C21–C26). However, in the anti configuration, the methyl group lies outside any such electronic influence.

By examining the ratio of the starting enolate and the aldol products in the reaction of **6** with acetophenone, we assume that the *Z* enolate gives the *anti* product, while the *E* enolate gives the *syn* aldol adduct.[16]

This relationship between the starting enolate and the final product requires a boatlike transition structure.[17] Although some reports indicated that it is possible to obtain the *anti* aldol product in reactions of the zirconium enolate of esters with aldehydes,[18] this fact was interpreted on the basis of a chair transition state. To the best of our knowledge, no report has appeared on the reactions of amide stereogenic zirconium enolates with ketones.

Previously Evans and McGee[9] have proposed that the *Z* $(cp)_2ZrCl_2$ enolates react with aldehydes *via* a chair-like transition state, whereas *E* enolates prefer to react *via* a boatlike transition state, with both the *E* and *Z* enolates affording *syn* aldol products. The isolation and structural characterization of **11** are our starting points for the discussion of the possible transition state involved in the reaction of **6** with acetophenone.

We assume that the reaction proceeds first *via* ketone complexation to the zirconium (we will see later in this article that the coordination of the carbonyl substrate to the zirconium is not the rate-determining step in this aldol condensation). We also assume that ketone complexation to the zirconium center is not linear, as shown

(16) Heathcock, C. H. In *Asymmetric Synthesis*; Morrison, D. J., Ed.; Academic: New York, 1984; Vol. 3, Chapter 2. Evans, D. A.; Nelson, J. V.; Taber, T. R. In *Topics in Stereochemistry*; Eliel, E. L., Wilen, S. H., Eds.; Wiley: New York, 1983; Vol. 13, p 1. Denmark, S. E.; Henke, B. R. *J. Am. Chem. Soc.* **1991**, *113*, 2177.

(17) Nakamura, E.; Kuwajima, I. *Tetrahedron Lett.* **1983**, 3343. Hoffmann, R. W.; Ditrich, K.; Froech, S. *Tetrahedron* **1985**, *41*, 5517. Nakamura, E.; Kuwajima, I. *Acc. Chem. Res.* **1985**, *18*, 181. Gennari, C.; Todeschini, R.; Beretta, M. G.; Favini, G.; Scolastico, C. *J. Org. Chem.* **1986**, *51*, 612.

(18) Sacha, H.; Waldmüller, D.; Braun, M. *Chem. Ber.* **1994**, *127*, 1959.

by spectroscopic,[19] computational,[19] and crystallographic[19,20] studies. In the case of aldehydes, theoretical calculations have shown that complexation of the Lewis acid *syn* to the aldehyde hydrogen atom is energetically favored.[19] In the case of ketones, spectroscopic studies[21] and calculations[19,22] have shown that complexation of the Lewis acid *syn* to the less sterically hindered group is less favored. The crystallographically observed conformation for **11** is half-chair. A force field calculation method recently developed[23] was able to generate structures of $(cp)_2MCl_2$ complexes (M = Ti, Zr) which are almost identical with those found by X-ray diffraction. However, the force field calculations have shown that clusters of energetically closely spaced conformations can exist which could accommodate reacting substrates. The isolated structure of **11** does not necessarily have the same conformation as that proposed for the transition state.[9] This notwithstanding, **11** does show some similarity with the transition structure, where the enolate, the carbonyl substrate, and the other zirconium substituents are in the same plane. This implies a rather acute O–Zr–O bond angle (75.4° in complex **11**). In a "normal" aldol reaction, the preferred chairlike structure for the idealized Zimmerman–Traxler cyclic transition state avoids vicinal nonbonding interactions. When an important steric interaction dominates, as in the case of the zirconium enolate for the presence of the bulky cp ring, the unfavorable eclipsing interactions in the boat transition structure are not energetically unfavorable. From this point of view, the cp zirconium enolate resembles the case of Denmark's recently calculated transition structure for five-coordinate silicon enolates.[24] The assumption that the aldolate product comes from the cyclic transition state is completely justified on the basis of our kinetic study (*vide infra*). In the case of the reaction of the *E* enolate **6** with acetophenone, we propose two possible transition structures, shown in Scheme 6.

Other conformations are surely possible and should be considered. The only way to distinguish the two transition structures is to calculate the energy difference between **A** and **B**. Steric interactions of the carbonyl substituents with the cp ring show that the twist-boat transition structure is favored, as also calculated by Denmark.[24] This naive view, however, does not consider the role of the bulky substituent groups on nitrogen and their interaction with the cp rings and the carbonyl substituent.

We have started to examine the possibility of an *ab initio* calculation on transition-metal enolates[25] and hope to address the question in the near future.

Mechanism of the Aldol Reaction. The structural characterization of cyclic **11** is, however, not enough to show that a cyclic transition state is encountered during this reaction. To address this question and to find the rate-determining step for the condensation, we undertook a kinetic study of complex **6** with acetophenone and *p*-substituted acetophenones.

Scheme 6

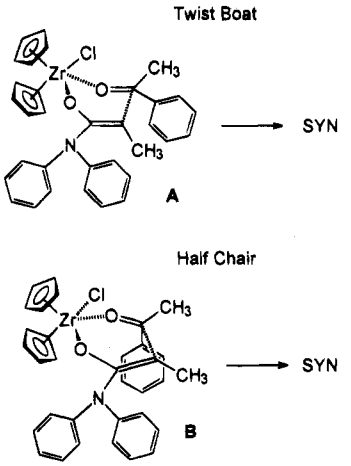

Table 3. Rate Constants from 300 to 340 K for the Reaction of 6 with Acetophenone in C_6D_6[a]

T (K)	k (M^{-1} h^{-1})	T (K)	k (M^{-1} h^{-1})
340	11.81 ± 0.07	310	3.05 ± 0.04
330	7.47 ± 0.08	300	1.66 ± 0.02
320	5.03 ± 0.06		

[a] $c_{10} = 2c_{20}$; $c_{20} = 0.1000$ M in all cases.

A kinetic study on the aldolic reaction promoted by silyl ketene acetals derived from amides was recently published,[26] and the authors reported activation parameters for the second-order reaction. The reaction is accelerated by electron-withdrawing groups, and a Hammett plot revealed that the rate-determining step is carbon–carbon bond formation. To the best of our knowledge, only one kinetic study on the aldolic reaction with a metal enolate has been performed previously, and this was conducted by our group on the aldolic condensation of acetophenone with $[\{(cp)_2Fe)CH(CH_2)O\}Zr(cp)_2Cl]$.[10b] However, the metal enolate used in this study, although useful for modeling purposes, does not find use in organic synthesis, unlike zirconium amide enolates.

The stereogenic zirconium enolate **6** was therefore allowed to react with acetophenone at five different temperatures, and the results are listed in Table 3.

On the basis of our previous explorations, we assume that the *Z* enolate gives rise to *anti* products, while *syn* compounds are formed from *E* enolates. Although we cannot exclude the possibility of cross-product (*i.e. Z* enolate giving *syn* product), it seems unlikely, given the constant mixture ratio observed during the course of the reactions. The reaction was monitored by recording the ratio of the integrals of the methyl peaks of **6** to those of **10**. The temperatures investigated were chosen so as to avoid overlap of the signals in question. The kinetic parameters derived for the conversion of the *Z* form of **6** into the *anti* diastereoisomer of **10**, and those for (*E*)-**6** into *syn*-**10**, were measured independently and found to be the same. An Eyring analysis of the reaction as a function of temperature gave the following results: $\Delta H^{\ddagger} = 38.3 \pm 0.9$ kJ mol^{-1}; $\Delta S^{\ddagger} \geq -181 \pm 3$ J

(19) Shambayati, S.; Crowe, W. E.; Schreiber, S. L. *Angew. Chem., Int. Ed. Engl.* **1990**, *29*, 256. Shambayati, S.; Schreiber, S. L. In *Comprehensive Organic Synthesis*; Schreiber, S. L., Ed.; Pergamon: Oxford, U.K., 1991; Vol. 1, p 283–324.
(20) Cozzi, P. G.; Floriani, C. Manuscript in preparation.
(21) Hartman, J. S.; Stilbs, P.; Forsens, S. *Tetrahedron Lett.* **1975**, *16*, 3497. Fratiello, A.; Stoner, C. S. *J. Org. Chem.* **1975**, *40*, 1244. Fratiello, A.; Kubo, R.; Chow, S. *J. Chem. Soc., Perkin Trans. 2* **1976**, 1205. Torri, J.; Azzaro, M. *Bull. Soc. Chim. Fr.* **1978**, 283.
(22) Goodman, J. M. *Tetrahedron Lett.* **1992**, *33*, 7219. Rauk, A.; Hunt, I. R.; Keay, B. A. *J. Org. Chem.* **1994**, *59*, 6808 and references therein.
(23) Doman, T. N.; Hollis, K. T.; Bosnich, B. *J. Am. Chem. Soc.* **1995**, *117*, 1352.
(24) Denmark, S. E.; Griedel, B. D.; Coe, D. M.; Schnute, M. E. *J. Am. Chem. Soc.* **1994**, *116*, 7026.
(25) Nottoli, R.; Sgamellotti, A.; Floriani, C. Unpublished results.
(26) Myers, A. G.; Kephart, S. E.; Chen, H. *J. Am. Chem. Soc.* **1992**, *114*, 7922. Myers, A. G.; Widdowson, K. L.; Kukkola, P. J. *J. Am. Chem. Soc.* **1992**, *114*, 2765.

Scheme 7

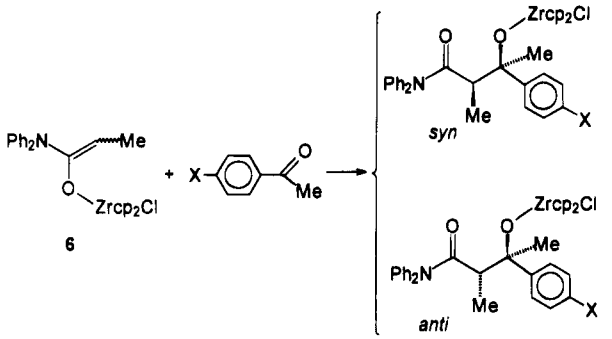

X = H, **10**
X = Me, **12a**
X = F, **12b**
X = Cl, **12c**
X = NO_2, **12d**

Table 4. Rate Constants from 300 to 340 K for the Reaction of 6 with *p*-Fluoroacetophenone in C_6D_6

T (K)	c_{20} (M)[a]	k (M^{-1} h^{-1})
340	0.0933	9.62 ± 0.30
330	0.0933	6.18 ± 0.10
330	0.0933[b]	5.74 ± 0.10
320	0.0933	3.75 ± 0.08
320	0.0933	3.52 ± 0.05
310	0.0933	2.19 ± 0.05
300	0.0933	1.08 ± 0.02

[a] $c_{10} = 2c_{20}$. [b] $c_{10} = 0.176$ M.

mol^{-1} K^{-1}; $\Delta G^{\ddagger}_{298} = 92.2 \pm 1.2$ kJ mol^{-1}. The entropy value is of the same order of magnitude as that reported by Myers and shows an ordered transition state, while the enthalpy of activation is lower than that of the aldol reaction of a silyl ketene acetal; in this latter example the coordination around the silicon must be disrupted in order to allow the binding to the electrophile. In our reaction the zirconium has an empty orbital available for the carbonyl substrate to bind to in the same plane as the amido enolate ligand, and any strain needed to accomplish the necessary geometry of the transition state is minimal.

As previously noted for acetophenone, **6** also reacts with a variety of *p*-substituted acetophenones to give mixtures of diastereoisomers (Scheme 7). In all cases significant deviations from the originally recorded ratio of 65:35 were not observed.

With 4-fluoroacetophenone the kinetic measurement was repeated at four different temperatures; results are collected in Table 4. A least-squares fit according to the Eyring equation gave the following activation parameters: $\Delta H^{\ddagger} = 43.5 \pm 1.3$ kJ mol^{-1}; $\Delta S^{\ddagger} \geq -167 \pm 4$ J mol^{-1} K^{-1}; $\Delta G^{\ddagger}_{298} = 93.3 \pm 1.8$ kJ mol^{-1}.

A kinetic study using other *p*-substituted acetophenones was carried out (Table 5). From the rates derived, we constructed a Hammett plot, which gave a positive ϱ value of 0.41. This is consistent with carbon−carbon bond formation as the rate-determining step and also confirms that, in general, electron-withdrawing substituents accelerate the rate. The point for *p*-nitroacetophenone does not correlate with the other points, presumably due to the complexation of the ketone as a process competing with the rate-determining steps as originally observed by Myers.[26]

In conclusion, our study, focusing on a widely used enolate for simple selection, represents the first complete presentation of the isolation and structural characterization of a zirconium amide enolate. It is hoped that the structural parameters can be used as a starting point to develop a theoretical model for the aldol reaction mediated by early transition metals. In addition, we have presented the first measurement of activation parameters for the aldolic reaction of a stereogenic enolate. The results obtained are consistent with the previously proposed cyclic transition state mechanism outlined at the beginning of this paper (Scheme 1).

Table 5. Rate Constants for the Reaction of 7 with Substituted *p*-Acetophenones in C_6D_6 at 320 K

c_{20} (M)[a]	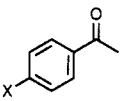	k (M^{-1} h^{-1})
0.0540	X = Me	2.37 ± 0.06
0.0933[b]	X = F	3.52 ± 0.05
0.0540	X = Cl	3.73 ± 0.09
0.0540	X = NO_2	9.37 ± 0.15
0.100[b]	X = H	5.03 ± 0.06

[a] $c_{10} = 3c_{20}$. [b] $c_{10} = 2c_{20}$.

Experimental Section

General Procedure. All reactions were carried out under an atmosphere of purified nitrogen. Solvents were dried and distilled before use by standard methods. Infrared spectra were recorded with a Perkin-Elmer 883 spectrophotometer, ^{1}H NMR spectra were measured on a 200-AC Bruker instrument.

Synthesis of *N,N*-Diphenylacetamide (1). Diphenylamine (23.82 g, 140 mmol) and acetyl chloride (5.53 g, 70 mmol) were dissolved in Et_2O (200 mL) and refluxed overnight. Diphenylamine hydrochloride was filtered off and the solution concentrated to 100 mL. The solution was left at 0 °C for a few days, and the crystallized amide was collected and used without further purification (85%). IR (Nujol): ν(C=O) 1671 cm^{-1}. Anal. Calcd for $C_{14}H_{13}NO$: C, 79.59; H, 6.20; N, 6.63. Found: C, 80.01; H, 6.34; N, 6.56. ^{1}H NMR (CD_2Cl_2): δ 2.03 (s, 3H, COMe), 7.3−7.5 (m, 10H, Ph).

Synthesis of *N,N*-Diphenylpropionamide (2). Diphenylamine (38.8 g, 288 mmol) and propionyl chloride (10 mL, 114 mmol) were dissolved in Et_2O (350 mL) and refluxed overnight. Diphenylamine hydrochloride was filtered off and the solvent evaporated to dryness, affording a white oil which crystallized after several days. The solid was washed with cyclohexane (50 mL), dried, and used without further purification (80%). IR (Nujol): ν(C=O) 1671 cm^{-1}. Anal. Calcd for $C_{15}H_{15}NO$: C, 79.97; H, 6.71; N, 6.22. Found: C, 80.34; H, 6.71; N, 6.48. ^{1}H NMR (CD_2Cl_2): δ 1.09 (t, 3H, J = 6.9 Hz, Me), 2.24 (q, 2H, J = 6.9 Hz, $COCH_2$), 7.2−7.5 (m, 10H, Ph).

Synthesis of 3. To an Et_2O (100 mL) solution of Pr^i_2NH (1.62 g, 160 mmol) was added a solution of BuLi in *n*-hexane (10 mL, 1.6 M, 16.0 mmol) at 0 °C. The solution was stirred for 20 min and then was cooled to −78 °C. To this ether solution of LDA was added a solution of **1** (3.38 g, 16.0 mmol) in THF (10 mL) over 1 h. After the addition the solution was warmed to room temperature, stirred for 1 h, and then stored at −20 °C. After a few days a white crystalline solid was formed, which was collected and dried under vacuum (81%). ^{1}H NMR (C_6D_6): δ 1.40 (m, 8H, THF), 3.42 (s, 1H, $=CH_2$), 3.63 (m, 9H, $=CH_2$, THF), 6.85−6.90 (m, 2H, Ph), 7.1−7.3 (m, 8H, Ph).

Synthesis of 5. To a solution of Pr^i_2NH (3.36 g, 32.3 mmol) in THF (150 mL) was added a solution of BuLi in *n*-hexane (20 mL, 32.0 mmol) at 0 °C, and the solution was stirred at the same temperature for 20 min. The LDA solution was cooled to −50 °C, and a solution of **1** (6.80 g, 32.2 mmol) in THF (50 mL) was slowly added over 1 h and stirred for another 30 min. To the clear solution was added $(cp)_2ZrCl_2$ (8.94 g,

30.6 mmol) in one portion. The yellow solution was stirred for 5–6 h and warmed to room temperature. The solvent was pumped off and the yellow solid collected with Et_2O. The solid was charged on a Soxhlet and extracted with mother liquor to afford, after 2 days, a yellow crystalline solid, which was filtered and collected (75%). Crystals suitable for X-ray analysis were obtained by extraction with Et_2O. Anal. Calcd for $C_{24}H_{22}ClNOZr$: C, 61.71; H, 4.75; N, 3.00. Found: C, 62.19, H, 4.75; N, 3.01. ^1H NMR (CD_2Cl_2): δ 3.64 (s, 2H, $=CH_2$), 6.22 (s, 10H, $Zr(cp)_2$), 7.0–7.4 (m, 10H, Ph). ^{13}C NMR (CD_2Cl_2): δ 78.1 ($=CH_2$), 115.1 ($Zr(cp)_2$), 123.5, 123.82, 125.15, 125.27, 129.54, 129.67 (Ph), 147.07 (Ph), 163.9 (COZr).

Synthesis of 6. To a solution of LDA (28.8 mmol) in THF (150 mL) at −60 °C was slowly added a solution of **2** (6.50 g, 28.85 mmol) in THF (50 mL), and this mixture was stirred at the same temperature for 1 h. To the clear solution was added $(cp)_2ZrCl_2$ (8.01 g, 27.4 mmol), and the mixture was warmed to room temperature with stirring over 6 h. The solvent was pumped off and the yellow solid collected with diethyl ether (60 mL). The solid was charged on a Soxhlet and extracted for 2 days with freshly distilled Et_2O. The yellow solid was collected and dried under vacuum (71%). X-ray-quality crystals were obtained by extraction with Et_2O. Anal. Calcd for $C_{25}H_{24}ClNOZr$: C, 62.41; H, 5.03; N, 2.91. Found: C, 62.35; H, 5.18; N, 2.83. ^1H NMR (CD_2Cl_2; two isomers, Z:E = 65:35): Z, δ 1.67 (d, 3H, J = 6.9 Hz, Me), 4.27 (q, 1H, J = 6.9 Hz, $=CHCH_3$), 6.14 (s, 10H, $(cp)_2Zr$), 7.0–7.4 (m, 10H, Ph); E, δ 1.43 (d, 3H, J = 6.8 Hz, Me), 4.56 (q, 2H, J = 6.8 Hz, $=CHCH_3$), 6.14 (s, $(cp)_2Zr$, 10H), 7.0–7.4 (m, 10H, Ph).

Synthesis of 7. A [$Cr(CO)_5(THF)$] solution prepared in situ by photolysis of $Cr(CO)_6$ (0.88 g, 4.0 mmol) in THF (250 mL) was added dropwise to a stirred solution of the complex **5** (1.64 g, 3.5 mmol) in THF (50 mL) at room temperature. The red solution was stirred for 5 h, and then the solvent was evaporated to dryness. To the oily residue was added Et_2O (80 mL), yielding a yellow crystalline solid, which was collected and dried (43%). Crystals suitable for X-ray analysis were obtained by extraction with Et_2O. IR (Nujol): ν(Cr(CO)) 2051 (w), 1938 (s), 1916 (s), 1840 (m) cm^{-1}. Anal. Calcd for $C_{29}H_{22}ClCrNO_6Zr$: C, 52.84; H, 3.36; N, 2.12. Found: C, 52.42; H, 3.14; N, 1.96. ^1H NMR (CD_2Cl_2): δ 1.72 (AB, 2H, J = 2.50 Hz, CH_2Cr), 6.28 (s, 5H, cp), 6.31 (s, 5H, cp), 7.3–7.5 (m, 10H, Ph). ^{13}C NMR (C_6D_6): δ 13.8 (CH_2Cr), 114.6 ($(cp)_2Zr$), 110–130 (Ph), 163.9 (NC–O), 191.3 (C–O), 219.8 (CrCO), 225.2 (CrCO).

Reaction of 5 with Benzaldehyde in a Sealed Tube. Synthesis of 8. Complex **5** (0.057 g, 0.12 mmol) and distilled benzaldehyde (0.012 mL, 0.12 mmol) were added to C_6D_6 in a NMR tube under nitrogen; then the solution was frozen and the tube sealed. After 2 h a ^1H NMR spectrum was recorded. ^1H NMR (C_6D_6): δ 2.42–2.93 (AB part of ABX, 2H, J_{AX} = 3.50 Hz, J_{BX} = 9.20 Hz, J_{AB} = 15.35 Hz, CH_2CO), 5.86 (s, 5H, $(cp)_2Zr$), 5.90 (X part of ABX, 1H, J_{AX} = 3.50 Hz, J_{BX} = 9.20 Hz, CHOZr), 6.18 (s, 5H, $(cp)_2Zr$), 6.8–7.3 (m, 15H, Ph).

Reaction of 5 with Acetophenone in a Sealed Tube. Synthesis of 10. Complex **5** (0.052 g, 0.11 mmol) and distilled acetophenone (0.013 mL, 0.11 mmol) were added to an NMR tube containing C_6D_6 under nitrogen; then the solution was frozen and the tube sealed. After 24 h a ^1H NMR spectrum was recorded. ^1H NMR (C_6D_6): δ 1.92 (s, 3H, Me), 2.79 (s, 2H, CH_2), 5.91 (s, 5H, $(cp)_2Zr$), 6.02 (s, 5H, $(cp)_2Zr$), 6.8–7.5 (m, 15H, Ph).

Reaction of 6 with Benzaldehyde in a Sealed Tube. Synthesis of 9. Complex **6** (0.054 g, 0.11 mmol) and distilled benzaldehyde (0.011 mL, 0.11 mmol) were added to an NMR tube containing CD_2Cl_2; then the solution was frozen and the tube sealed. After 24 h a ^1H NMR spectrum was recorded. ^1H NMR (CD_2Cl_2); two diastereoisomers, *syn*:*anti* = 81:19): *syn*, δ 1.38 (d, 3H, J = 6.7 Hz, Me), 2.70 (m, 1H, CHMe), 5.12 (d, 1H, J = 9.1 Hz, CH–O), 6.11 (s, 5H, cp), 6.28 (s, 5H, cp), 6.7–7.5 (m, 15H, Ph); *anti*, δ 0.76 (d, 3H, J = 6.9 Hz), 2.92 (m, 1H, CHMe), 5.20 (d, 1H, J = 9.0 Hz, CH–O), 6.01 (s, 5H, cp), 6.35 (s, 5H, cp), 6.75–7.5 (m, 15H, Ph).

Reaction of 6 with Acetophenone in a Sealed Tube. Synthesis of 10. Complex **6** (0.046 g, 0.09 mmol) and distilled acetophenone (0.011 mL, 0.09 mmol) were added to an NMR tube containing C_6D_6; then the solution was frozen and the tube sealed. After 24 h a ^1H NMR spectrum was recorded. ^1H NMR (C_6D_6; two diastereoisomers, *syn*:*anti* = 37:67): *syn*, δ 1.51 (d, 3H, J = 6.91 Hz, Me), 1.97 (s, 3H, Me), 3.05 (q, 2H, J = 6.91 Hz, CH_2), 5.81 (s, 5H, $(cp)_2Zr$), 6.16 (s, 5H, $(cp)_2Zr$), 6.8–7.5 (m, 15H, Ph); *anti*, δ 0.93 (d, 3H, J = 7.07 Hz), 1.88 (s, 3H), 3.21 (q, 1H, J = 7.07 Hz), 5.86 (s, 10H, $(cp)_2Zr$), 6.8–7.5 (m, 15H, Ph). IR (Nujol): ν(CO) 1664 cm^{-1}.

Synthesis of 11. The zirconium enolate **6** (1.61 g, 3.35 mmol) was added to a solution of distilled acetophenone (0.41 g, 3.40 mmol) in CH_2Cl_2 (50 mL), and the yellow solution was stirred overnight. To the resulting pale yellow solution was added dropwise a solution of silver triflate (0.88 g, 3.40 mmol) in CH_3CN (20 mL). The solution turned colorless, and AgCl was filtered off after 30 min of stirring. The solvent was pumped off, and to the resulting oil was added Et_2O (50 mL). The mixture was stirred, yielding a white crystalline solid, which was filtered and dried. Crystals suitable for X-ray analysis were obtained from an extraction with 5:1 Et_2O/dimethoxyethane. Anal. Calcd for $C_{34}H_{32}FNO_5SZr$: C, 57.12; H, 4.51; N, 1.96. Found: C, 57.17; H, 4.78; N, 2.26. ^1H NMR (CH_2Cl_2); two isomers, *syn*:*anti* = 35:65): *syn*, δ 0.90 (d, 3H, J = 7.12 Hz, Me), 1.68 (s, 3H, Me), 3.00 (q, 1H, J = 7.12 Hz, CH), 6.12 (s, 10H, $(cp)_2Zr$), 7.15–7.60 (m, 15H, Ph); *anti*, δ 1.35 (s, 3H, Me), 1.48 (d, 3H, J = 6.97 Hz), 3.18 (q, 1H, J = 6.97 Hz), 5.95 (s, 10H, $(cp)_2Zr$), 7.15–7.60 (m, 15H, Ph). IR (Nujol): ν(CO) 1590 cm^{-1}.

X-ray Crystallography for Complexes 6, 7, and 11. The crystals selected for study were mounted in glass capillaries and sealed under nitrogen. The reduced cells were obtained with use of TRACER.[27] Crystal data and details associated with data collection are given in Tables 1 and S1 (Table S1 is in the supporting information). Data were collected at room temperature (295 K) on a single-crystal diffractometer. For intensities and background the profile measurement technique was used.[28] The structure amplitudes were obtained after the usual Lorentz and polarization corrections,[29] and the absolute scale was established by the Wilson method.[30] The crystal quality was tested by ψ scans, showing that crystal absorption effects could not be neglected. Data were then corrected for absorption using the program ABSORB.[31] The function minimized during the least-squares refinement was $\sum w|\Delta F|^2$. Unit weights were used for all complexes, since these gave a satisfactory analysis of variance and the best agreement factors.[29] Anomalous scattering corrections were included in all structure factor calculations.[32b] Scattering factors for neutral atoms were taken from ref 32a for non-hydrogen atoms and from ref 33 for H atoms. Solution and refinement were based on the observed reflections.

Complex 6. The structure was solved using SHELX86.[34] Refinement was first done isotropically, and then anisotropically for non-hydrogen atoms, by full-matrix least squares. The hydrogen atoms were located from difference Fourier maps and introduced in the subsequent refinements as fixed-atom contributions with isotropic U's fixed at 0.10 Å^2. During the

(27) Lawton, S. L.; Jacobson, R. A. TRACER (a Cell Reduction Program); Ames Laboratory, Iowa State University of Science and Technology: Ames, IA, 1965.
(28) Lehmann, M. S.; Larsen, F. K. *Acta Crystallogr., Sect. A: Cryst. Phys. Diffr., Theor. Gen. Crystallogr.* **1974**, *A30*, 580.
(29) Data reduction, structure solution, and refinement were carried out on an IBM AT personal computer equipped with an INMOS T800 transputer using: Sheldrick, G. SHELX-76: System of Crystallographic Computer Programs; University of Cambridge: Cambridge, England, 1976.
(30) Wilson, A. J. C. *Nature* **1942**, *150*, 151.
(31) Ugozzoli, F. *Comput. Chem.* **1987**, *11*, 109.
(32) (a) *International Tables for X-ray Crystallography*; Kynoch Press: Birmingham, England, 1974; Vol. IV, p 99. (b) *Ibid.*, p 149.
(33) Stewart, R. F.; Davidson, E. R.; Simpson, W. T. *J. Chem. Phys.* **1965**, *42*, 3175.
(34) Sheldrick, G. SHELX-86: Program for the Solution of Crystal Structures; University of Göttingen, Göttingen, Germany, 1986.

refinement the phenyl and cyclopentadienyl rings were constrained to be regular hexagons (C–C = 1.395 Å) and pentagons (C–C = 1.42 Å), respectively. Since the space group is polar, the crystal chirality was tested by inverting all the coordinates ($x, y, z \rightarrow -x, -y, -z$) and refining to convergence once again. The resulting R values ($R = 0.026$, $R_G = 0.028$ *vs* $R = 0.027$, $R_G = 0.029$) indicated that the original choice should be considered the correct one.

Complex 7. The structure was solved by the heavy-atom method starting from a three-dimensional Patterson map. Refinement was first done isotropically, and then anisotropically for non-hydrogen atoms, by full-matrix least squares. The hydrogen atoms were located from difference Fourier maps and introduced in the subsequent refinements as fixed-atom contributions with isotropic U's fixed at 0.12 Å^2 for those associated to the cyclopentadienyl rings and C29 methyl and 0.06 Å^2 for the remainders.

Complex 11. The structure was solved by the heavy-atom method starting from a three-dimensional Patterson map. Refinement was done by full-matrix least squares first isotropically, and then anisotropically for non-hydrogen atoms, except for the S1N, F1A, F1B, F2A, and O4A, and O4B atoms of the $CF_3SO_3^-$ anion and for the THF solvent molecule. The $CF_3SO_3^-$ anion was found to be affected by a severe disorder. The best fit was obtained by considering the S1, O4, F1, and F2 atoms distributed over two positions (A and B) with the site occupation factors given in Table S4 (supporting information). Attempts to split the F3 fluorine atom in two positions were unsuccessful. The THF solvent molecule (O6, C61–C64) was found to be statistically distributed over two positions around an inversion center. The hydrogen atoms were put in geometrically calculated positions and introduced in the last stage of refinement as fixed-atom contributions with isotropic U's fixed at 0.10 Å^2. The H atoms associated with the disordered THF molecule were ignored. During the refinement the phenyl and cyclopentadienyl rings were constrained to be regular hexagons (C–C = 1.395 Å) and pentagons (C–C = 1.42 Å), respectively. Some constraints were also applied to distances within the THF molecule.

The final difference maps showed no unusual features, with no significant peak above the general background. Final atomic coordinates are listed in Tables S2–S4 for non-hydrogen atoms and in Tables S5–S7 for hydrogens (supporting information). Thermal parameters are given in Tables S8–S10 and bond distances and angles in Tables S11–S13 (supporting information).[35]

Kinetics. Kinetic measurements were obtained by ^{1}H NMR in deuterated benzene at 300, 310, 320, 330, and 340 K. Measurements at 310 K have been made twice with the same concentration and once with a lower concentration. Values of rate constants are reproducible to within 5% error. Relative concentrations of starting and final products are measured with the integration of the doublet of the methyne proton for the couple *Z–anti* in **6** and **10** at 1.67 and 0.93 ppm, respectively, and for the couple *E–syn* at 1.43 and 1.51 ppm, respectively. Integrations of both peak couples give very accurate values with a general difference of 1–2%.

Reaction 1 has been carried out by mixing **6** and acetophenone in the NMR tube at low temperature (~220 K).

(35) See paragraph at the end of the paper regarding supporting information.

$$\mathbf{6} + \text{acetophenone} \xrightarrow{k} \mathbf{10}\ (\text{or}\ \mathbf{12}) \qquad (1)$$

The reaction was started by heating the sample up to the desired temperature. Since this heating process in the NMR spectrometer does not proceed like a unit step function, the time at which $t = 0$ cannot be determined precisely. For this reason, unequal initial concentrations of the reactants were chosen, *viz.* c_{10} (=[acetophenone]) = $2c_{20}$ (=2[**6**]), and the time at the estimated $t = 0$ was set to t_0, a parameter that will be optimized by the least-squares fitting procedure. This ensures that the evaluation of the rate constant k does not depend on the more or less arbitrarily chosen time scale. Integration of the differential equations describing reaction 1 yields eq 2.

$$[\mathbf{10}]\ (\text{or}\ [\mathbf{12}]) = c_{20} - \frac{c_{10} - c_{20}}{\frac{c_{10}}{c_{20}} e^{(c_{10}-c_{20})k(t-t_0)} - 1} \qquad (2)$$

The parameters c_{10}, c_{20}, and t_0 are defined above, t is the time in hours, and k is the second-order rate constant in M^{-1} h^{-1}. Since the relative concentration of **10** (or **12**) in percent (percentage of **10** or of **12**) is available with a minimum error, k and t_0 were evaluated *via* a least-squares analysis according to eq 3.

$$\%\ \mathbf{10}\ (\text{or}\ \%\ \mathbf{12}) = 100\left[1 - \frac{c_{10} - c_{20}}{c_{10} e^{(c_{10}-c_{20})k(t-t_0)} - c_{20}}\right] \qquad (3)$$

The rate constants at various temperatures are given in Tables 3 and 4. The concentration of acetophenone, c_{10}, is (2–3)c_{20}.

Activation parameters are calculated by a $1/\sigma^2$ weighted least-squares fit according to the transition state theory (eq 4), where $\kappa = 1$ if the probability is 100% that the transition state does not give the starting materials, k_B is the Boltzmann constant and is 1.38×10^{-23} J K^{-1}, h is Planck's constant and is 6.63×10^{-34} J Hz^{-1}, and $R = 8.314$ J mol^{-1} K^{-1}. The

$$k = \kappa k_B \frac{T}{h} \exp\left\{\frac{-\Delta H^{\ddagger}}{RT}\right\} \exp\left\{\frac{\Delta S^{\ddagger}}{R}\right\} \qquad (4)$$

following parameters were obtained: $\Delta S^{\ddagger} \geq -181 \pm 3$ J mol^{-1} K^{-1}, $\Delta H^{\ddagger} = 38.3 \pm 0.9$ kJ mol^{-1}, $\Delta G^{\ddagger}_{298} = 92.2 \pm 1.2$ kJ mol^{-1} and $\Delta S^{\ddagger} \geq -167 \pm 4$ J mol^{-1} K^{-1}, $\Delta H^{\ddagger} = 43.5 \pm 1.3$ kJ mol^{-1}, $\Delta G^{\ddagger}_{298} = 93.3 \pm 1.8$ kJ mol^{-1} for the reaction of **6** with acetophenone or *p*-fluoroacetophenone, respectively (see Tables 3 and 4).

Acknowledgment. We thank the "Fonds National Suisse de la Recherche Scientifique" (Grant No. 20-40268.94) and Ciba-Geigy (Basel, Switzerland) for financial support.

Supporting Information Available: Tables giving crystal data and details of the structure determination, fractional atomic coordinates, anisotropic thermal parameters, bond lengths, and bond angles for complexes **6**, **7**, and **11** (14 pages). Ordering information is given on any current masthead page.

OM9505017